Dual Time Point ^{18}F-FDG PET Imaging for Differentiating Malignant from Inflammatory Processes

Hongming Zhuang, Michael Pourdehnad, Eric S. Lambright, Alvin J. Yamamoto, Michael Lanuti, Peiyong Li, P. David Mozley, Milton D. Rossman, Steven M. Albelda, and Abass Alavi

Divisions of Nuclear Medicine, Thoracic Surgery, and Pulmonary Medicine, Hospital of the University of Pennsylvania, Philadelphia, Pennsylvania

The aim of this study was to investigate the difference in the rates of FDG uptake between malignant and inflammatory cells and processes. **Methods:** In vitro studies: ^{18}F-FDG uptake by different tumor cell lines (human mesothelioma [REN]; rat mesothelioma [II45]; mice melanoma [B18F10]; mice mesothelioma [AB12]; human myeloma [GM1500]; and human ovarian cancer [SKOV3]) and peripheral blood mononuclear cells isolated from 8 healthy human volunteers was measured 20 and 60 min after FDG was added into growth medium. Animal studies: II45 cells were implanted into the left flank of rats ($n = 5$) and a focal inflammatory reaction (mechanical irritation) was generated in the right flank. PET images at 45 and 90 min after injection of FDG were obtained and standardized uptake values (SUVs) were determined. Patient studies: Seventy-six patients who had dual time FDG PET scans were retrospectively analyzed. All results were expressed as the percentage change in SUV of the later time image from that of the earlier time (mean ± SD). **Results:** In vitro studies: Except for the SKOV3 cell line, which had only minimally increased FDG uptake (+10% ± 26%; $P > 0.3$), all other tumor cell lines tested showed significantly increased FDG uptake over time (GM1500, +59% ± 19%; B18F10, +81% ± 15%; AB12, 93% ± 21%; II45, +161% ± 21%; REN, +198% ± 48%; $P < 0.01$ for all). By contrast, FDG uptake in mononuclear cells was decreased in 7 of 8 donors. Animal studies: SUVs of tumors from 90-min images were significantly higher than those from 45-min images (+18% ± 8%; $P < 0.01$), whereas the SUVs of inflammatory lesions decreased over time (−17% ± 13% of the early images; $P < 0.05$). Clinical studies: The SUVs of delayed images from the known malignant lesions compared with those of earlier scans increased over time (+19.18% ± 9.58%; $n = 31$; $P < 0.001$; 95% confidence interval, 15.8%–22.6%). By contrast, the SUVs of benign lung nodules decreased slightly over time (−6.3% ± 8.1%; $n = 12$; $P < 0.05$; 95% confidence interval, −10.9% to −1.7%). The SUV of inflammatory lesions caused by radiation therapy (+1.16% ± 7.23%; $n = 8$; $P > 0.05$; 95% confidence interval, −3.9%–6.2%) and the lesions of painful lower limb prostheses (+4.03% ± 11.32%; $n = 25$; $P > 0.05$; 95% confidence interval, −0.4%–8.5%) remained stable over time. **Conclusion:** These preliminary data show that dual time imaging appears to be useful in distinguishing malignant from benign lesions. Further research is necessary to confirm these results.

Key Words: PET; FDG; dual time point imaging; malignancy; inflammation; standardized uptake value

J Nucl Med 2001; 42:1412–1417

Functional and metabolic imaging is rapidly evolving into a major discipline in the management of patients with cancer. Many reports indicate that ^{18}F-FDG PET is sensitive and specific in the diagnosis and staging of several types of malignancies (*1*). Malignant cells, in general, show increased glucose utilization (*2*), probably caused by an increased number of glucose transporter proteins (*3*) and increased enzyme levels of hexokinase and phosphofructokinase promoting glycolysis (*4*). As a result, FDG uptake, which reflects glucose metabolic rate, is increased in cancer cells.

FDG accumulation is not specific to tumors. There are numerous causes of FDG uptake in benign processes seen on FDG PET images (*5*). Increased uptake of FDG at the suspected sites of inflammation and infection is used to detect a variety of inflammatory and infectious disorders (*6,7*). The increased FDG uptake in the unknown benign lesions also gives rise to false positive results when a patient is managed for a potential malignant disorder. This results in a decreased positive predictive value of the test in such settings (*8*). Because various cell types exhibit varying rates of FDG uptake, we hypothesized that determination of these measurements at 2 time points may prove to be of value in differentiating malignant from benign processes in the unknown and thus enhancing specificity of FDG PET. Therefore, this investigation was undertaken to assess the potential role of dual time point FDG PET imaging.

Received Dec. 18, 2000; revision accepted May 14, 2001.

For correspondence or reprints contact: Abass Alavi, MD, Division of Nuclear Medicine, Hospital of the University of Pennsylvania, 110 Donner Building, 3400 Spruce St., Philadelphia, PA 19104.

MATERIALS AND METHODS

Cell Culture

Human peripheral blood mononuclear cells (PBMCs) were isolated from 8 healthy donors using Ficoll methods (*9*). Malignant cells, which included human malignant mesothelioma cell line (REN), rat malignant mesothelioma cell line (II45), mice malignant melanoma (B18F10), mice mesothelioma (AB12), human myeloma (GM1500), and human ovarian cancer (SKOV3) were handled as previously described (*10–14*). Only freshly isolated PBMCs and exponentially growing cancer cells were used in experiments. Attached cells were dissociated with 0.05% trypsin-0.02% ethylenediaminetetraacetic acid. Viable cell number was assessed by the trypan blue dye exclusion technique. All experiments were conducted in a humidified incubator containing 5% CO_2 at 37°C.

FDG Uptake Studies

FDG was diluted in RPMI media (*15*) (Sigma, St. Louis, MO) to obtain a final concentration of 37 kBq (1 μCi)/10 μL 250,000 (2.5×10^5). Viable cells (0.1 mL) in RPMI containing 100 mg/dL glucose were aliquoted into a 96-well V-bottom cell culture plate (Costar Corp., Cambridge, MA). FDG (0.037 MBq [1 μCi]) was added to the cells and incubation continued for 20–60 min. The cells were washed 4 times with phosphate-buffered solution. Radioactivity was measured by β-counting. FDG uptake was expressed as counts per minute per million viable cells. The FDG uptake was conducted at least 4 times for each type of cell or each human donor and the average level of uptake was obtained. Statistical comparisons were based on Student's *t* test and $P < 0.05$ was considered to be statistically significant.

Animal Preparation and FDG PET Imaging

Five male Fisher-344 rats were used for this study. One million II45 cells were implanted into the left flank of each rat 2 wk before the PET study. Three days before imaging, a focal inflammatory reaction was generated in the right flank of the animals by local incision and suture placement. The animals were fasted for 4 h and administered 4.81 MBq/kg (130 μCi/kg) FDG intravenously. PET images of the entire body were obtained 45–90 min after injection using the UGM HEAD PET scanner (UGM-ADAC Inc., Philadelphia, PA) (*16*). This scanner encompasses an imaging volume of 256-mm diameter in the transverse direction and 256 mm in the axial direction. The data were reconstructed into a $128 \times 128 \times 128$ matrix, with $(2\text{-mm})^3$ cubic voxel; thus, the images could be viewed as 128 slices in the transaxial, sagittal, or coronal plane. The spatial resolution of the system was 3.5 mm in both transverse and the axial direction. The attenuation-corrected filtered back-projected images were used for both visual and quantitative analysis. The maximum standardized uptake value (SUV), obtained by selecting a small region of interest (ROI), was used in analysis. Partial volume correction was not performed. Results are expressed as percentage change in SUV in the respective lesions between early and late images. Body weight correction method (*17*) was used for generating SUVs in this study:

$$\text{SUV} = \frac{\text{Tissue activity (mCi/mL)}}{\text{Injected FDG dose (mCi)/body weight (kg)}}.$$

Patient Studies

Seventy-six patients (35 men, 41 women; age range, 45–77 y; mean age, 64 y) who had undergone dual time FDG PET scans and had confirmed specific pathologic lesions or at least 9 mo of clinical follow-up were retrospectively analyzed. These included 31 patients with malignant lesions (25 with lung cancer; 2 with mesothelioma; 2 with non-Hodgkin's lymphoma; 1 with esophageal cancer; 1 with lung metastasis from breast cancer); 12 patients with surgical pathology confirmed ($n = 10$) or clinical follow-up suggested ($n = 2$); benign lung nodules that showed clinically significant FDG uptake (4 with granuloma; 1 with tuberculosis; 1 with Mycobacterium avium-intracellulare infection; 1 with sarcoidosis; 3 with unclear diagnosis but no tumor cells seen on surgical pathology examination; 2 with a nodule that had stablized or disappeared upon follow-up CT); 8 with inflammation caused by radiation; and 25 with painful lower limb prostheses (24 of them with loosening and 1 with periprosthetic infection; 19 confirmed by revision surgery and 5 based on follow-up results). PET scans were acquired using the C-PET scanner (UGM-ADAC). None of the patients with malignancy had received chemotherapy or radiation therapy before the FDG PET scan. All patients fasted for ≥4 h before PET scanning. Data acquisition began 48–63 min after the intravenous injection of 2.516 MBq/kg (0.068 mCi/kg) FDG. The average interval between the first time point and the second time point acquisition was 52 min (41–65 min). After injection, singles transmission scans were obtained over the entire area scanned using a ^{137}Cs point source (*18*). The images were reconstructed using the ordered subsets-expectation maximization method (*19*). A small ROI consisting of 4 pixels, which revealed the maximum SUV of the lesion, was carefully drawn. Results are expressed as percentage change in SUV of the index lesion between early and late images.

RESULTS

In Vitro Studies

All tumor cells tested had increased FDG uptake over time (from +10% ± 26% for SKOV3 to +198% ± 48% for REN) (Table 1). By contrast, FDG uptake in mononuclear cells decreased over time in 7 of 8 donors with an average decrease of 13% (Table 2).

Animal Studies

The SUVs of tumors from delayed images were significantly higher than those from early images (+18% ± 8%, $P < 0.01$). The average SUV of tumors from early image was 3.49, whereas the average SUV from delayed images was 4.12. By contrast, the SUVs of the inflammatory lesions

TABLE 1
Changes of In Vitro FDG Uptake over Time by Malignant Cells

Cell name	Cell type	Species	Average change (%)	SD (%)	*P*
B18F10	Melanoma	Mouse	+81	15	<0.01
AB12	Mesothelioma	Mouse	+93	12	<0.01
II45	Mesothelioma	Rat	+161	21	<0.01
REN	Mesothelioma	Human	+198	48	<0.01
GM1500	Myeloma	Human	+59	19	<0.01
SKOV3	Ovarian cancer	Human	+10	26	>0.05
	All malignant		+100.3		

TABLE 2
Changes of In Vitro FDG Uptake over Time by Inflammatory Cells

Patient no.	Cell type	Species	Average change (%)	SD (%)	*P*
1	Mononuclear	Human	−17	4	<0.01
2	Mononuclear	Human	−29	4	<0.01
3	Mononuclear	Human	−7	3	<0.05
4	Mononuclear	Human	−10	5	<0.05
5	Mononuclear	Human	−44	6	<0.01
6	Mononuclear	Human	−18	2	<0.01
7	Mononuclear	Human	+27	7	<0.05
8	Mononuclear	Human	−6	1	<0.05
	All benign		−13		

decreased over time (−17% ± 13% of the early images; $P < 0.05$). The average SUV of inflammatory lesions from the early images was 2.33, whereas the average SUV from delayed images was 1.93 (Fig. 1).

Patient Studies

The average SUV of the lesions in known cancer patients increased from 3.96 at the first time point to 4.72 at the second time point (+19.2% ± 9.6%; $n = 31$; $P < 0.001$) (Fig. 2). By contrast, the average SUV of benign lung nodules slightly decreased over time from 2.37 to 2.22 (−6.3% ± 8.1%; $P < 0.05$; $n = 12$). The SUVs of inflammatory lesions caused by radiation therapy remained almost constant over time (+1.2% ± 7.2%; $n = 8$; $P > 0.05$). In this group of patients, the average SUV changed from 2.56 at the first time point to 2.59 at the second time point. Similarly, the SUVs of lesions of painful lower limb prostheses were also relatively stable over time, with average SUV changing from 2.61 to 2.71 (+4.0% ± 11.3%; $n = 25$; $P > 0.05$). The results of the in vivo studies are summarized in Table 3.

DISCUSSION

Distinguishing malignant from benign inflammatory/infectious process is challenging because both can show increased FDG uptake. Traditionally, a threshold for a single time point SUV of 2.5–3.8 has been proposed as the optimal threshold for separating malignant from benign lung lesions (*20,21*). Subsequently, this threshold also was used by many groups to diagnose other malignancies. However, there is considerable overlap between SUVs of malignant and benign lesions, causing difficulty in correctly interpreting FDG PET data. There is a wide range of FDG uptake among malignant lesions. For example, non–small cell lung carcinoma has an average SUV of 8, whereas the average SUV for breast cancer is only 3 (*22*). Sugawara et al. (*6*) reported that the SUV of infectious lesions could be as high as 6.69. We have also observed high SUVs in inflammatory and infectious lesions. For example, most periprosthetic infections have relatively high SUVs, ranging from 3 to 6, whereas sarcoid lesions can have SUVs as high as 11. Reports describing the fact that inflammatory and infectious lesions or benign variations can simulate malignant lesions are numerous (*8,23,24*). Consequently, SUVs at single time points alone may not be reliable enough to characterize malignant lesions of various organ systems (*25,26*). Therefore, the investigation of alternative methods using FDG PET for differentiation of malignant from benign lesions is warranted.

In a study using a turpentine-induced inflammation model on rats, Yamada et al. (*27*) found that FDG uptake in inflammatory tissue increased gradually until 60 min after injection and then decreased gradually. The time course of FDG uptake by malignant cells is less clear based on what is published in the literature. Although initiating an FDG PET image at 50–60 min after injection is common practice in staging lung cancer and appears quite successful, this procedure may not be optimal for other tumor types, especially in settings where benign inflammatory lesions are of a clinical concern. There is, however, increasing evidence suggesting that tumor uptake of FDG increases for hours after injection. In a study of 8 patients with stage III lung cancer, Hamberg et al. (*28*) first found that FDG uptake by tumor did not reach the maximum level until approximately 5 h after injection. Lodge et al. (*29*) reported that significant differences were observed in the time–activity response of benign and high-grade tumors in 29 patients with soft-tissue masses. They found that FDG uptake by high-grade sarcoma reaches a peak at approximately 4 h after injection, whereas benign lesions do so within 30 min.

Our experimental approach included an in vitro system, a small tumor-bearing animal model, and clinical patient studies. The properties of these systems were inherently different. For example, the blood–tumor barrier was not accounted for in the in vitro experiment. Furthermore, im-

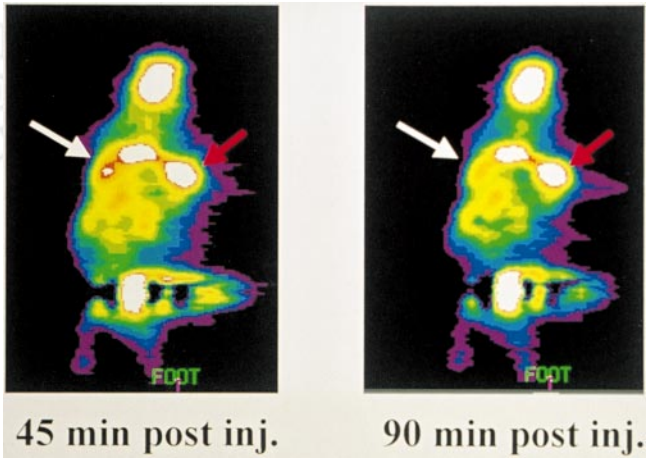

FIGURE 1. Coronal images of same rat at early and late time point. White arrow points to inflammatory lesion; red arrow points to malignant lesion. Compared with early time point, SUV of inflammatory lesion in later time point decreased 25% and SUV of malignant lesion increased 16%. inj = injection.

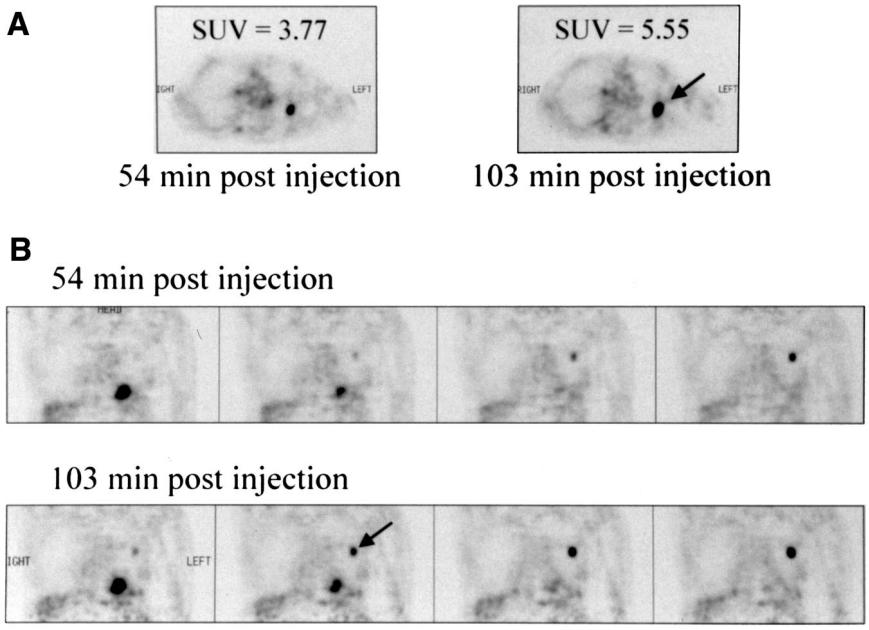

FIGURE 2. Comparison of early and delayed FDG PET images from 61-y-old man with lung carcinoma: transaxial images (A) and coronal images (B). Arrow points to lesion. Malignant focus became more apparent in later images and SUV increased from 3.77 to 5.55.

planted tumors and inflammation from surgical trauma in animal models are different from spontaneous neoplasms and inflammatory processes in patients. Despite these variables, our results from these 3 distinct systems were consistent.

We chose mononuclear cells over granulocytes for our in vitro experiment. Mononuclear cells, which include monocytes and lymphocytes, are the major inflammatory cell population involved in chronic infections and inflammation, whereas granulocytes are the main inflammatory cells involved in acute infections. Both granulocytes and mononuclear cells have increased glucose utilization at the site of infection. However, acute infection is rarely confused with malignancy in FDG PET studies because of distinct clinical presentation and other findings. In contrast, chronic inflammation or infection, such as granuloma or tuberculosis, can frequently cause diagnostic dilemma in interpreting FDG PET results. Therefore, we felt that investigation of the difference in FDG uptake patterns between mononuclear cells and malignant cells was more likely to provide clinically relevant information.

Our in vitro experiments showed that all tumor cell lines had different degrees of increased FDG uptake over time, whereas the mononuclear cells isolated from 7 human donors showed different degrees of decreased FDG uptake over time. Apparently, this phenomenon cannot be simply interpreted by basic pharmacokinetics to indicate that FDG accumulation will increase in cells when FDG concentration in the media remain constant, because it cannot explain why FDG uptake by mononuclear cells did not increase in our experiments, considering that both types of cells were in identical experiment conditions. Our data showed that uptake of FDG by mononuclear cells was indeed different from that of most tumor cells tested. These results provided evidence, on a cellular level, that dual time point imaging may be an effective way to distinguish malignant from benign lesions with FDG PET imaging.

Other authors have used similar methods but with different radiopharmaceuticals in differentiating benign from malignant lesions. In a study involving 57 patients who had SPECT images of the brain at 30 min and 3 h after intravenous administration of ^{99m}Tc(V)-DMSA, Hirano et al.

TABLE 3
Changes of SUVs Over Time in Animal Experiment and Clinical Studies

Type of lesion	Species	Average 1st SUV	Average 2nd SUV	Average change (mean ± SD%)	95% Confidence interval
Experimental malignancy	Rat	3.49	4.12	+18 ± 8	+10.99% to +25.01%
Experimental inflammation	Rat	2.33	1.93	−17 ± 13	−28.39% to −5.61%
Clinical malignant	Human	3.92	4.76	19.18 ± 9.58	+15.81% to +22.55%
Benign lung nodule	Human	2.37	2.22	−6.30 ± 8.09	−10.88% to −1.72%
Radiation reaction	Human	2.56	2.59	1.16 ± 7.27	−3.88% to +6.20%
Painful lower leg prosthesis	Human	2.61	2.71	4.03 ± 11.32	−0.40% to +8.46%

(*30*) showed that the delayed uptake ratio, retention ratio, and retention index were higher in the malignant tumors than the benign tumors. Similarly, based on the information from early and delayed SPECT brain images obtained at about 10 min and 3 h, respectively, after intravenous injection of ^{201}Tl, Sun et al. (*31*) concluded that the radioactivity was stable or decreased slightly in benign or low-grade tumors (average retained index, 0.96 ± 0.24), whereas the radioactivity was increased in high-grade or metastatic tumors.

It is unclear why inflammatory and malignant lesions exhibit a differential FDG uptake pattern over time. Several factors may contribute to this phenomenon on a cellular basis. Although it is well known that many cancer cells express increased numbers of glucose transporters (Glut1) (*32*), metabolic trapping through phosphorylation of FDG appears more likely as the rate-determining step in FDG retention in the cells. Hexokinase and glucose-6-phosphatase mediate the phosphorylation and dephosphorylation of intracellular FDG, respectively. Unless FDG-6-phosphate is dephosphorylated by glucose-6-phosphatase, it is unable to leave the cell. Furthermore, it has been shown that most actively proliferating tumor cells have low levels of glucose-6-phosphatase (*33*,*34*). Based on this observation, an increased ratio of hexokinase/glucose-6-phosphatase in tumors may result in gradual accumulation of FDG-6-phosphate. By contrast, most normal tissues express greater levels of glucose-6-phosphatase than malignant cells. Mononuclear cells, which represent the major cell population in chronic inflammation and infection, express high levels of glucose-6-phosphatase (*35*) and, therefore, have a relatively low ratio of hexokinase/phosphatase. Consequently, in mononuclear cells, FDG-6-phosphate can be rapidly dephosphorylated and cleared after reaching a certain level. Thus, the differential ratio of hexokinase/phosphatase may contribute to the distinct FDG uptake observed between inflammatory and malignant lesions over time. However, on the whole-body level, there are more factors complicating this issue. For example, different blood vessel density between malignant and inflammatory lesions can have a dramatic influence on FDG uptake. Dynamic image and compartmental model analysis (*36*) may be an appropriate next step to further understand dual time imaging.

Varying levels of glucose-6-phosphatase activity among different tumor cell types may also explain the wide range of FDG retention over time. Tumor types with lower glucose-6-phosphatase activity are more likely to be detected by dual time point FDG PET imaging than those with higher levels of this enzyme. The majority (87.1%) of the malignant lesions in our clinical studies were either nonsmall cell lung carcinoma or mesothelioma. These cell types appear to maintain high FDG uptake rates at the later time point. Our in vitro study showed that FDG uptake by ovarian cancer cells (SKOV3) did not show a significant increase over time. Interestingly, ovarian cancers have been found to express a relatively low ratio of hexokinase/phosphatase (*37*). This may explain why our SKOV3 cells behaved differently when compared with other types of malignant cells. In any case, further basic and clinical investigations are necessary to determine which malignant disorders are best suited to dual time point imaging with FDG PET.

The results of our human studies were consistent with the results of our in vitro and animal experiments. Because of the small reaction volume in the in vitro study, nearly all of the FDG added into media was immediately available to cells. In contrast, only a small fraction of injected FDG reached the lesions at any given time in animal and human studies. To account for this difference in availability of FDG, we measured in vitro FDG uptake at a much earlier time point than in the animal and human studies. It was disappointing, but not surprising, to see that some benign lesions also exhibited increased SUVs over time, and, conversely, that not all malignant lesions revealed increasing SUVs over time. However, it should be noted that the 95% confidence intervals of the percentage change in FDG uptake over time for malignant and benign lesions did not overlap.

Our in vitro tests and animal experiments were well controlled and conducted under uniform conditions. However, a considerable degree of variation was seen among patients. Uptake of FDG in benign lesions can be influenced by underlying etiology (infection vs. inflammation) and state of inflammation (acute vs. chronic). Differences in FDG uptake may also be related to the different inflammatory cells involved and the extent of activation of these cells. Furthermore, it can be influenced by individual physiologic and immunologic status, which may account for the increased FDG uptake observed in 1 of 8 sets of donated mononuclear cells, whereas the remaining 7 showed decreased uptake. In malignant lesions, even among the same histologic type of tumors that presumably have the similar ratio of hexokinase/glucose-6-phosphatase, the combination of coexisting chronic or acute inflammation, necrosis, hypoxia, and degree of angiogenesis can all complicate the pattern of FDG uptake. For example, hypoxia can increase FDG uptake by tumor cells caused by increased anaerobic glycolytic pathway (*2*,*38*).

The time interval between the early and delayed scans can also affect the accuracy of dual time point imaging (*39*). Several earlier studies suggested that there could be higher sensitivity for detecting malignancy when the images were obtained at 3–5 h instead of at 1 h (*28*,*29*,*40*). Our results indicated that the SUV changes over shorter intervals (average, 52 min) between the first and the second data acquisition provided sufficient information for the interpretation of FDG PET images. Because FDG uptake by inflammatory cells reaches its peak at about 60 min, the time interval between tracer injection and first scan is also likely to be a factor that may affect the performance of this technique. In addition, medical intervention, such as chemotherapy or radiation therapy, might affect the effectiveness of dual time point imaging. None of the patients with malignancy in our

study had received therapy for their tumors. Therefore, more studies need to be conducted to assess whether dual time point imaging can be as effective in evaluating post-therapy patients as in pretherapy patients.

CONCLUSION

Based on the data presented, it appears that lung lesions with decreased or stable SUVs over time are likely to have a benign etiology. In contrast, lung lesions with increased SUVs over time are likely to be caused by malignancy. The other types of malignant lesions studied may also show the same pattern, but no conclusions can be made from the limited data available. Although more studies are necessary to further our understanding of this technique, dual time point imaging is a potentially promising method in FDG PET imaging for distinguishing malignant from benign lesions. The SUV, both initially and over time (for difficult cases), may provide a better way to differentiate benign and malignant lesions in FDG PET imaging.

ACKNOWLEDGMENT

The authors are grateful to the late Dr. Robin J. Smith for his assistance in generating quantitative data for this project.

REFERENCES

1. Rigo P, Paulus P, Kaschten BJ, et al. Oncological applications of positron emission tomography with fluorine-18 fluorodeoxyglucose. *Eur J Nucl Med*. 1996;23:1641–1674.
2. Pauwels EK, Ribeiro MJ, Stoot JH, McCready VR, Bourguignon M, Maziere B. FDG accumulation and tumor biology. *Nucl Med Biol*. 1998;25:317–322.
3. Flier JS, Mueckler MM, Usher P, Lodish HF. Elevated levels of glucose transport and transporter messenger RNA are induced by ras or src oncogenes. *Science*. 1987;235:1492–1495.
4. Monakhov NK, Neistadt EL, Shavlovskil MM, Shvartsman AL, Neifakh SA. Physicochemical properties and isoenzyme composition of hexokinase from normal and malignant human tissues. *J Natl Cancer Inst.* 1978;61:27–34.
5. Bakheet SM, Powe J. Benign causes of 18-FDG uptake on whole body imaging. *Semin Nucl Med*. 1998;28:352–358.
6. Sugawara Y, Braun D, Kison P, Russo J, Zasadny K, Wahl R. Rapid detection of human infections with fluorine-18 fluorodeoxyglucose and positron emission tomography: preliminary results. *Eur J Nucl Med*. 1998;25:1238–1243.
7. Zhuang HM, Duarte PS, Pourdehand M, Shnier D, Alavi A. Exclusion of chronic osteomyelitis with F-18 fluorodeoxyglucose positron emission tomographic imaging. *Clin Nucl Med*. 2000;25:281–284.
8. Strauss LG. Fluorine-18 deoxyglucose and false-positive results: a major problem in the diagnostics of oncological patients. *Eur J Nucl Med.* 1996;23:1409–1415.
9. Kay HD. A new procedure to overlay diluted blood on Ficoll-Hypaque gradients. *J Immunol Methods*. 1980;39:81–83.
10. Evans CE, Ward C, Rathour L, Galasko CB. Myeloma affects both the growth and function of human osteoblast-like cells. *Clin Exp Metastasis*. 1992;10:33–38.
11. Davis MR, Manning LS, Whitaker D, Garlepp MJ, Robinson BWS. Establishment of a murine model of malignant mesothelioma. *Intl J Cancer*. 1992;52:881–886.
12. Kozbor D, Lagarde AE, Roder JC. Human hybridomas constructed with antigen-specific Epstein-Barr virus-transformed cell lines. *Proc Natl Acad Sci USA*. 1982;79:6651–6655.
13. Fidler IJ. Selection of successive tumour lines for metastasis. *Nature*. 1973;242:148–149.
14. Fogh J, Wright WC, Loveless JD. Absence of HeLa cell contamination in 169 cell lines derived from human tumors. *J Natl Cancer Inst.* 1977;58:209–214.
15. Moore GE, Woods LK. Culture media for human cells: RPMI 1630, RPMI 1634, RPMI 1640 and GEM 1717. *Tissue Culture Assoc Manual*. 1976;3:503–508.
16. Karp JS, Freifelder R, Geagan MJ, et al. Three-dimensional imaging characteristics of the HEAD PENN-PET scanner. *J Nucl Med*. 1997;38:636–643.
17. Kim CK, Gupta NC, Chandramouli B, Alavi A. Standardized uptake values of FDG: body surface area correction is preferable to body weight correction. *J Nucl Med*. 1994;35:164–167.
18. Karp JS, Muehllehner G, Qu H, Yan XH. Singles transmission in volume-imaging PET with a ^{137}Cs source. *Phys Med Biol*. 1995;40:929–944.
19. Bedigian MP, Benard F, Smith RJ, Karp JS, Alavi A. Whole-body positron emission tomography for oncology imaging using singles transmission scanning with segmentation and ordered subsets expectation maximization (OS-EM) reconstruction. *Eur J Nucl Med.* 1998;25:659–661.
20. Patz EF Jr, Lowe VJ, Hoffman JM, et al. Focal pulmonary abnormalities: evaluation with F-18 fluorodeoxyglucose PET scanning. *Radiology*. 1993;188:487–490.
21. Hubner KF, Buonocore E, Gould HR, et al. Differentiating benign from malignant lung lesions using "quantitative" parameters of FDG PET images. *Clin Nucl Med*. 1996;21:941–949.
22. Torizuka T, Zasadny KR, Recker B, Wahl RL. Untreated primary lung and breast cancers: correlation between F-18 FDG kinetic rate constants and findings of in vitro studies. *Radiology*. 1998;207:767–774.
23. Cook GJ, Maisey MN, Fogelman I. Normal variants, artefacts and interpretative pitfalls in PET imaging with 18-fluoro-2-deoxyglucose and carbon-11 methionine. *Eur J Nucl Med.* 1999;26:1363–1378.
24. Kato T, Fukatsu H, Ito K, et al. Fluorodeoxyglucose positron emission tomography in pancreatic cancer: an unsolved problem. *Eur J Nucl Med*. 1995;22:32–39.
25. Hustinx R, Smith RJ, Benard F, Bhatnagar A, Alavi A. Can the standardized uptake value characterize primary brain tumors on FDG-PET? *Eur J Nucl Med.* 1999;26:1501–1509.
26. Zhuang HM, Duarte PS, Pourdehnad M, Li PY, Alavi A. Standardized uptake value as an unreliable index of renal disease on FDG-PET imaging. *Clin Nucl Med*. 2000;25:358–360.
27. Yamada S, Kubota K, Kubota R, Ido T, Tamahashi N. High accumulation of fluorine-18-fluorodeoxyglucose in turpentine-induced inflammatory tissue. *J Nucl Med*. 1995;36:1301–1306.
28. Hamberg LM, Hunter GJ, Alpert NM, Choi NC, Babich JW, Fischman AJ. The dose uptake ratio as an index of glucose metabolism: useful parameter or oversimplification? *J Nucl Med*. 1994;35:1308–1312.
29. Lodge MA, Lucas JD, Marsden PK, Cronin BF, O'Doherty MJ, Smith MA. A PET study of ^{18}FDG uptake in soft tissue masses. *Eur J Nucl Med.* 1999;26:22–30.
30. Hirano T, Otake H, Kazama K, et al. Technetium-99m(V)-DMSA and thallium-201 in brain tumor imaging: correlation with histology and malignant grade. *J Nucl Med*. 1997;38:1741–1749.
31. Sun D, Liu QC, Liu WG, Hu WW. Clinical application of Tl-201 SPECT imaging of brain tumors. *J Nucl Med*. 2000;41:5–10.
32. Younes M, Lechago LV, Somoano JR, Mosharaf M, Lechago J. Wide expression of the human erythrocyte glucose transporter Glut1 in human cancers. *Cancer Res.* 1996;56:1164–1167.
33. Gallagher BM, Fowler JS, Gutterson NI, MacGregor RR, Wan CN, Wolf AP. Metabolic trapping as a principle of radiopharmaceutical design: some factors responsible for the biodistribution of [^{18}F]2-deoxy-2-fluoro-D-glucose. *J Nucl Med*. 1978;19:1154–1161.
34. Nelson CA, Wang JQ, Leav I, Crane PD. The interaction among glucose transport, hexokinase, and glucose-6-phosphatase with respect to 3H-2-deoxyglucose retention in murine tumor models. *Nucl Med Biol*. 1996;23:533–541.
35. Suzuki S, Toyota T, Suzuki H, Goto Y. Partial purification from human mononuclear cells and placental plasma membranes of an insulin mediator which stimulates pyruvate dehydrogenase and suppresses glucose-6-phosphatase. *Arch Biochem Biophys*. 1984;235:418–426.
36. Fischman AJ, Alpert NM. FDG-PET in oncology: there's more to it than looking at pictures. *J Nucl Med*. 1993;34:6–11.
37. Minn H, Kangas L, Knuutila V, Paul R, Sipila H. Determination of 2-fluoro-2-deoxy-D-glucose uptake and ATP level for evaluating drug effects in neoplastic-cells. *Res Exp Med*. 1991;191:27–35.
38. Clavo AC, Wahl RL. Effects of hypoxia on the uptake of tritiated thymidine, L-leucine, L-methionine and FDG in cultured cancer cells. *J Nucl Med*. 1996;37:502–506.
39. Hustinx R, Smith RJ, Benard F, et al. Dual time point fluorine-18 fluorodeoxyglucose positron emission tomography: a potential method to differentiate malignancy from inflammation and normal tissue in the head and neck. *Eur J Nucl Med.* 1999;26:1345–1348.
40. Boerner AR, Weckesser M, Herzog H, et al. Optimal scan time for fluorine-18 fluorodeoxyglucose positron emission tomography in breast cancer. *Eur J Nucl Med.* 1999;26:226–230.

JNM The Journal of NUCLEAR MEDICINE

Dual Time Point ^{18}F-FDG PET Imaging for Differentiating Malignant from Inflammatory Processes

Hongming Zhuang, Michael Pourdehnad, Eric S. Lambright, Alvin J. Yamamoto, Michael Lanuti, Peiyong Li, P. David Mozley, Milton D. Rossman, Steven M. Albelda and Abass Alavi

J Nucl Med. 2001;42:1412-1417.

The Journal of Nuclear Medicine is published monthly.
SNMMI | Society of Nuclear Medicine and Molecular Imaging
1850 Samuel Morse Drive, Reston, VA 20190.
(Print ISSN: 0161-5505, Online ISSN: 2159-662X)

SNMMI SOCIETY OF NUCLEAR MEDICINE AND MOLECULAR IMAGING